Korea-Australia Rheology Journal
Vol. 20, No. 2, June 2008 pp. 51-58

Processing parallel-disk viscometry data in the presence of wall slip

Yee-Kwong Leong[1,*], Graeme R. Campbell[2], Y. Leong Yeow[3] and John W. Withers[3]
[1]*School of Mechanical Engineering, The University of Western Australia, Crawley, Western Australia, Australia 6009*
[2]*School of Engineering, James Cook University, Townsville, Queensland, Australia 4811*
[3]*Department of Chemical and Biomolecular Engineering, The University of Melbourne, Victoria, Australia 3010*
(Received March 4, 2008; final revision received April 3, 2008)

Abstract

This paper describes a two-step Tikhonov regularization procedure for converting the steady shear data generated by parallel-disk viscometers, in the presence of wall slip, into a shear stress-shear rate function and a wall shear stress-slip velocity functions. If the material under test has a yield stress or a critical wall shear stress below which no slip is observed the method will also provide an estimate of these stresses. Amplification of measurement noise is kept under control by the introduction of two separate regularization parameters and Generalized Cross Validation is used to guide the selection of these parameters. The performance of this procedure is demonstrated by applying it to the parallel disk data of an oil-in-water emulsion, of a foam and of a mayonnaise.

Keywords : wall slip velocity, apparent shear rate, ill-posed problem, Tikhonov regularization, integral equation

1. Introduction

Most of the commonly encountered methods for converting steady-shear viscometry data, such as the pressure drop versus flow rate data from capillary viscometers or the torque versus rotational speed data from Couette and parallel-disk viscometers, into a shear stress versus shear rate material property function $\tau(\dot{\gamma})$ assume the no-slip boundary condition where the material under test meets the walls of the viscometer. For some rheologically complex materials, the no-slip boundary condition may not be a good description of the physical conditions prevailing at such boundaries. For example, for some polymer melts, when the wall shear stress is sufficiently high physical slippage at the wall may be observed. For some concentrated suspensions or emulsions, slippage may be the consequence of the formation of a low viscosity film next to the wall which then serves as a lubricating layer resulting in what is known as apparent slip. In either case, the breakdown of the no-slip boundary condition greatly complicates the treatment of the viscometry data. See Yoshimura and Prud'homme (1988).

A number of specialized techniques have been developed to deal with such complications and to extract from such data not only the shear stress function $\tau(\dot{\gamma})$ but also a second material property function, the slip velocity function $v_s(\tau_w)$, that describes the variation of the slip velocity with wall shear stress τ_w. Examples of such techniques include the well-established Mooney (1931) procedure for different viscometers, the various methods proposed by Schlegel (1980), Yoshimura and Prud'homme (1988), Kiljañski (1989) and Wein and Tovchigrechko (1992), for Couette viscometry. Some of the methods for Couette viscometers require specially selected radius ratios for the outer and inner cylinders. Yoshimura and Prud'homme (1988) developed a method specifically for converting the parallel disk data from two different disk gaps into $\tau(\dot{\gamma})$ and $v_s(\tau_w)$. All these methods are used by rheologists to cope with wall slip. Yeow and coworkers (2003, 2004) have shown how the Tikhonov regularization procedures developed for processing capillary and Couette viscometry data without slip can be modified to allow for real or apparent wall slip.

Converting the torque versus rotational speed Γ-ω data of parallel-disk viscometer into material property functions poses a particular difficult problem even in the absence of wall slip. This is because of the significant variation of shear rate between the centre of the disk and the rim of the disk. In commercial instruments, this is often sidestepped by assuming that the material under test can be treated as a Newtonian liquid so that the shear stress varies linearly from the centre to the rim of the disks. For some highly shear thinning fluids or fluid with yield stress this can lead to errors as large as 20 to 30% which was recently reported by Yeow and coworkers (2007). Tikhonov regularization is able to convert parallel-disk viscometry data, in the absen-

*Corresponding author: leong@mech.uwa.edu.au

ce of wall slip, into a $\tau(\dot{\gamma})$ curve without making the Newtonian assumption as shown by Yeow and coworkers (2005). For parallel disk data that exhibit real or apparent slip, as indicated by the dependence of the data on the disk gap h, this method can still be applied but the resulting $\tau(\dot{\gamma})$ is now dependent on h. Such $\tau(\dot{\gamma})$ functions are not material property function and are referred to as shear stress-apparent shear rate functions $\tau(\dot{\gamma}_{App})$. The method of Yoshimura and Prud'homme mentioned above is an algebraic procedure that converts a pair of gap-dependent $\tau(\dot{\gamma}_{App})$ functions into a $\tau(\dot{\gamma})$ curve and a $v_{slip}(\tau_w)$ curve. To cope simultaneously with the $\tau(\dot{\gamma}_{App})$ functions from three or more disk gaps the Mooney method is usually used. This is essentially a graphical technique in which the apparent shear rate at the rim of the disks $\dot{\gamma}_{AppR}$ for different disk gaps, at a selected constant rim shear stress τ_R, is plotted as a linear function of the reciprocal of disk gap 1/h. The slip velocity v_s and true shear rate $\dot{\gamma}$ at the selected τ_R are then deduced from the slope of the linear plot and from the intercept when 1/h is extrapolated to zero.

There is another complication associated with the treatment of the Γ-ω data of parallel-disk viscometers that may be amplified by wall slip and needs to be addressed. Most of the procedures used to process these Γ-ω data assume that the azimuthal component v_θ is the only significant velocity component, *i.e.*, the ratio of the radial and the azimuthal velocity component $v_r/v_\theta \ll 1$ within the parallel-disk flow field. In the absence of wall slip, it is further assumed that v_θ is given by a simple expression of the form

$$v_\theta(r,z) = \frac{\omega r z}{h} \tag{1}$$

reported in Mascosko (1994) where v_θ is linear in both r and z. The validity of these kinematic assumptions can be checked by using FEM computation to solve the full equation of motion within the parallel-disk flow field. The FEM results of Shipman and coworkers (1991) show that, under conditions relevant to parallel-disk viscometry, *i.e.*, low Reynolds number and small gap to radius ratio $h/R \ll 1$, the assumption that $v_r/v_\theta \ll 1$ is valid and the v_θ is indeed approximately linear in r and in z and can be described to a high degree of accuracy by Eq. (1). When there is slippage at the disk walls, the situation becomes considerably more complex and all the kinematic simplifications need to be reassessed. Firstly, it is necessary to verify that the condition $v_r/v_\theta \ll 1$ remains valid. Recent FEM simulation results reported by Yeow and coworkers (2006), based on a number of assumed but realistic wall slip functions and a typical shear thinning viscosity function, show that, provided the inertia term can be ignored and $h/R \ll 1$, then the condition $v_r/v_\theta \ll 1$ is met. The FEM results also show that v_θ remains approximately linear in z and can be approximated by an expression of the form

$$v_\theta(r,z) = \left(\frac{\omega r z}{h} - \frac{2v_{slip}(\tau_w(r))z}{h}\right) + v_{slip}(\tau_w(r)) \tag{2}$$

reported by Yoshimura and Prud'homme (1988) and Brunn (1998).

The linearity in z is important as it is central to the method of Yoshimura and Prud'homme for obtaining the slip velocity function. However, these recent FEM results also reveal that v_θ and consequently τ_w, in general, can no longer be treated as a linear or even approximately linear function of r. As mentioned above, nonlinear variation of τ_W with r for non-Newtonian fluids, even when there is no wall slip, is a source of error in the processing of the Γ-ω data generated by parallel-disk viscometers. Yeow and coworkers (2006) showed that this error can become significantly amplified by wall slip thereby making the Newtonian assumption unacceptable.

This paper describes a general numerical procedure for converting the Γ-ω data, from an arbitrary number of disk gap $N_G \geq 2$, into $\tau(\dot{\gamma}_{App})$ curves and then into $\tau(\dot{\gamma})$ and $v_{slip}(\tau_w)$ material property functions. It does not rely on the linearity or approximate linearity of the wall shear stress in r. The conversion covers the entire range of the shear stress, from the lowest shear stress at the centre of the disks to the maximum rim shear stress of the multi-gap data. The procedure is based on two sequential applications of Tikhonov regularization. In the first application, essentially that described in Yeow and coworkers (2005), Tikhonov regularization is used to solve an integral equation of the first kind to convert the Γ-ω data into $\dot{\gamma}(\tau_{App})$ curve-one curve for each disk gap. In the second application it is used to solve a set of algebraic equations to convert the multiple $\dot{\gamma}(\tau_{App})$ curves into material property functions $\dot{\gamma}(\tau)$ and $v_{slip}(\tau_w)$. Thus the combination of these two applications of Tikhonov regularization forms a two-step procedure for converting parallel disk data, in the form of torque versus rotational speed Γ-ω for different disk gaps, into $\dot{\gamma}(\tau)$ and $v_{slip}(\tau_w)$ property curves.

As the first application of Tikhonov regularization is described in Yeow and coworkers (2005) only a brief description of this will be included. Attention will be focused on the second application of Tikhonov regularization. In this paper the selection of the regularization parameter, in both of the Tikhonov regularization steps, will be guided by the method of Generalized Cross Validation (GCV) described in Wahba (1990) instead of the Morozov Principle described in Engl and coworkers (2000) used by Yeow and coworkers. This new development will be outlined. The overall performance of the present way of handling parallel-disk viscometry data with wall slip will be demonstrated by applying it to three sets of laboratory data.

2. Integral equation and shear stress-apparent shear rate curves

Following existing practice, the Γ-ω data are converted into apparent rim shear rate at the rim $\dot{\gamma}_{AppR}$ versus Γ where $\dot{\gamma}_{AppR}=\omega R/h$ and R is the radius of the disks. Subscript App is used to highlight that, because of wall slip, wR/h is the apparent shear rate at the rim and the $\dot{\gamma}_{AppR}$-Γ data for different h do not fall on a single curve. Thus for each h the data take the form $(\dot{\gamma}_{AppR1}=\mathrm{Min}(\dot{\gamma}_{AppR}), \Gamma_1^M)$, $(\dot{\gamma}_{AppR2}, \Gamma_2^M)$, $\ldots(\dot{\gamma}_{AppRi}, \Gamma_i^M)$,... $\ldots(\dot{\gamma}_{AppRN_D}=\mathrm{Max}(\dot{\gamma}_{AppR}), \Gamma_{N_D}^M)$. N_D is the number of data points. Superscript M denotes experimentally measured quantities. These data are converted to $\tau(\dot{\gamma}_{App})$ by solving the integral equation of the first kind that relates the torque at any rotational speed to $\tau(\dot{\gamma}_{App})$

$$\Gamma^C=\frac{2\pi R^3}{\dot{\gamma}_{AppR}^3}\int_0^{\dot{\gamma}_{AppR}}\tau(\dot{\gamma}_{App})\dot{\gamma}_{App}^2 d\dot{\gamma}_{App} \tag{3}$$

as given in Mascosko (1994). Superscript C is used to distinguish the computed torque from its experimentally measured counterpart. The lower limit of the integral in Eq. (3) is exactly zero because at the centre of the disks the shear rate, with or without wall slip, vanishes identically. Thus the solution of this equation gives the shear stress at $\dot{\gamma}_{App}=0$. If this stress is not equal to zero, it is taken to be the finite shear stress at which the material first begins to yield or to exhibit wall slip. This is in direct contrast to existing methods of obtaining $\tau(\dot{\gamma}_{App})$ which are based on the expression given by Yoshimura and Prud'homme (1988),

$$\tau_R=\frac{\Gamma}{2\pi R^3}\left[3+\frac{d\log_e\Gamma}{d\log_e\dot{\gamma}_{AppR}}\right] \tag{4}$$

that relates the rim shear stress τ_R to the measured torque Γ and to its derivative with respect to $\dot{\gamma}_{AppR}$. Apart from the difficulties associated with noise amplification caused by numerical approximation of the derivative, this expression is also unable to provide any information about τ for $0\le\dot{\gamma}_{App}<\mathrm{Min}(\dot{\gamma}_{AppR})$. (Note: in invoking the Newtonian approximation the derivative term on the RHS of Eq. (4) is replaced by unity). The computational steps used in Yeow and coworkers (2005) for solving Eq. (3) is summarised in the next paragraph.

The span of the experimental data, $0\le\dot{\gamma}_R\le\dot{\gamma}_{RMax}$, is divided into N_K points at uniformly spaced interval $\Delta=\dot{\gamma}_{RAppN_D}/(N_K-1)$ apart with $N_K>>N_D$. Typically, N_K is of the order of 201 to 601. The corresponding discretized $\tau(\dot{\gamma}_{App})$ is represented by the unknown column vector $\tau=\{\tau_1, \tau_2, \tau_3,\ldots\tau_j,..\tau_{N_K}\}$. In terms of these discretized variables Eq. (3) becomes

$$\Gamma_i^C=\frac{2\pi R^3}{\dot{\gamma}_{AppRi}^3}\sum_{j=1}^{N_K}\alpha_{ij}\tau_j\dot{\gamma}_{Appj}^2\Delta,\ 1\le i\le N_D \tag{5a}$$

where α_{ij} are known numerical coefficients arising from the discretization of the integral in Eq. (3). Eq. (5a) can be represented compactly by

$$\Gamma^C=A\tau \tag{5b}$$

where $A_{ij}=2\pi R^3\alpha_{ij}\dot{\gamma}_{Appj}^2\Delta/(\dot{\gamma}_{AppRi}^3)$. The elements of the unknown column vector τ are chosen so that they: (i) minimize the sum of squares of the difference between the measured and computed column vectors of the torque $(\Gamma^M-\Gamma^C)$ and (ii) minimize the sum of squares of the second derivative of $d^2\tau/d\dot{\gamma}_{App}^2$ at the internal discretization points, $2\le j\le N_K-1$ to ensure a smooth $\tau(\dot{\gamma}_{App})$. In Tikhonov regularization, a linear combination of (i) and (ii) is minimized. The τ that does this is given by

$$\tau=\left(A^TA+\frac{\lambda}{\Delta^4}\beta^T\beta\right)^{-1}A^T\Gamma^M \tag{6}$$

according to Engl and coworkers (2000). β is the tri-diagonal matrix with rows of the general form (0, 0,.....0, 1, −2, 1, 0,.....0, 0) arising from the standard finite difference approximation of the second derivative $d^2\tau/d\dot{\gamma}_{App}^2$. λ is the adjustable regularization parameter. A large λ favors condition (ii) giving a smooth $\tau(\dot{\gamma}_{App})$. On the other hand, a small λ favors (i) and ensures a close match between Γ^M and Γ^C but may result in a $\tau(\dot{\gamma}_{App})$ that exhibits excessive and physically unreal fluctuations.

3. Regularization parameter based on GCV

Yeow and coworkers (2005) used the Morozov Principle described in Engl and workers (2000) to guide the selection of λ. In this method λ is adjusted so that the average difference between Γ^M and Γ^C is comparable with the expected average error bar of the viscometry data. This method has the advantage that the appropriate λ can be located requiring only a relatively small amount of computation. It may, however, involve a certain amount of subjective judgment if the average error bar is not known with sufficient certainty or when the error bars vary greatly from data point to data point.

The method of GCV described in Wahba (1990) used here to guide the selection of λ is based on the "leaving-out-one" principle. The computation described by Eq. (6) is, in principle, repeated N_D times each time leaving out one data point. The sum of squares V(λ) of the difference between the predicted value and the actual value for each of the left out data point clearly depends on λ. The optimum λ_{opt} is taken to be the minimizer of V(λ). In the GCV implementation of the "leaving-out-one" principle, V(λ) is given by

$$V(\lambda)=\frac{(\Gamma^M-\Gamma^C)^T(\Gamma^M-\Gamma^C)/N_D}{(1-\mathrm{Tr}[\mathbf{B}]/N_D)^2}. \tag{7}$$

Tr[**B**] denotes the trace of the square matrix **B**, known as the influence matrix, defined by

$$\mathbf{B}=\mathbf{A}(\mathbf{A}^T\mathbf{A}+\frac{\lambda}{\Delta^4}\beta^T\beta)^{-1}(\mathbf{A})^T. \quad (8)$$

Eqs. (5) and (6) together with the definition of **A**, β and **B** allow $V(\lambda)$ to be evaluated and plotted against λ/Δ^4. Finally the λ_{opt} that minimizes $V(\lambda)$ is substituted into Eq. (6) to give the discretized approximation of $\tau(\dot{\gamma}_{App})$. This step is repeated for the Γ-ω data for each disk gap.

4. Apparent shear rate and material property functions

To convert the discretized $\tau(\dot{\gamma}_{App})$, one for each disk gap, into material property functions it is more convenient to treat the apparent shear rate as a function of shear stress, *i.e.*, $\dot{\gamma}_{App}(\tau)$. Since Eq. (6) gives τ at a large number of regularly spaced $\dot{\gamma}_{App}$, it is a simple operation to invert $\tau(\dot{\gamma}_{App})$, for each disk gap, to $\dot{\gamma}_{gApp}(\tau)$, $g=1, 2, \ldots N_G$. Subscript g is used to denote the apparent shear rate curve associated with disk gap h_g.

At a given stress, the apparent shear rate $\dot{\gamma}_{gApp}(\tau)$ is the combined result of the actual shear rate experienced by the material $\dot{\gamma}(\tau)$ and the slippage velocity $v_{slip}(\tau)$ at the top and the bottom disks. Linear dependence of v_θ on z allows Eq. (2) to be rewritten, according to Yoshimura and Prud'homme (1988), as

$$\dot{\gamma}^C_{gApp}(\tau)=\dot{\gamma}(\tau)+\frac{2v_s(\tau)}{h_g},\ 2\le g\le N_G \quad (9)$$

Parallel disk data are usually reported for a small number of disk gaps, typically, $2\le N_G\le 8$. Superscript C is again used to distinguish the computed apparent shear rate based on Eq. (9) from that based on Eq. (6). Eq. (9) has to be satisfied at a series of selected stress $\tau_g=\{\tau_{g1}, \tau_{g2},. \tau_{gi_m} .. \tau_{gM}\}$, *i.e.*, the column vector $\dot{\gamma}^C_{gApp}$ should approximate $\dot{\gamma}_{gApp}(\tau)$ at each element of τ_g and for all the disk gaps $\mathbf{h}=\{h_1, h_2,\ldots h_g,\ldots h_{N_G}\}$. M is the number of uniformly distributed points covering the range of stress spanned by each of the $\dot{\gamma}_{gApp}(\tau)$ curves from Eq. (6). Typically M=15 to 25 points for each $\dot{\gamma}_{gApp}(\tau)$, $1\le g\le N_G$ and if necessary M can be varied for different g to allow for the variation in the range of τ associated with different $\dot{\gamma}_{gApp}(\tau)$ curves.

For the special case of $N_G=2$, Eq. (9) can be treated as two algebraic equations and solved to give the two material property functions explicitly

$$\dot{\gamma}(\tau)=\frac{h_1\dot{\gamma}_{App1}(\tau)-h_2\dot{\gamma}_{App2}(\tau)}{(h_1-h_2)},$$

$$v_s(\tau_w)=\frac{h_1h_2[\dot{\gamma}_{2App}(\tau_w)-\dot{\gamma}_{1App}(\tau_w)]}{2(h_1-h_2)}. \quad (10)$$

These are the expressions developed by Yoshimura and Prud'homme (1988) and now routinely used in the analysis of parallel disk data exhibiting wall slip. For $N_G>2$, Eq. (10) can, in principle, be applied to one pair of the apparent shear rate curves at a time to give the corresponding material property functions. This will result in multiple sets of material property functions which may or may not be in satisfactory agreement with one another.

To cope with the general case of multiple gaps, $N_G\ge 2$, the present investigation adopts a different approach. The range of stress $\tau_{min}\le\tau\le\tau_{max}$ covered by the complete set of $\dot{\gamma}_{gApp}(\tau)$ is discretized into $\sigma=\{\sigma_1=\tau_{min}, \sigma_2,\ldots \sigma_{N_p}=\tau_{max}\}$ where $N_P>>N_G\times M$ is some appropriately chosen number. σ is used here in place of τ to distinguish this known discretized stress vector from the unknown stress vector in Eq. (3). The unknown $\dot{\gamma}(\tau)$ and $v_{slip}(\tau)$ are represented by the column vectors $\dot{\gamma}=\{\dot{\gamma}_1, \dot{\gamma}_2,\ldots\dot{\gamma}_{N_p}\}$ and $\mathbf{v}_{slip}=\{v_{slip1}, v_{slip2},\ldots v_{slipN_p}\}$ at the discretization points of σ. From Eq. (9), the computed apparent shear rate for any disk gap $\dot{\gamma}_{gApp}$ is given by

$$\dot{\gamma}^C_{gApp\ i_m}=\sum_{i_p}^{N_p}C_{gi_mi_p}\dot{\gamma}_{i_p}+\frac{2}{h_g}\sum_{i_p}^{N_p}D_{gi_mi_p}v_{slip\ i_p}$$

$i_m=1, 2,\ldots M,\ g=1, 2,\ldots N_G.$ (11a)

Or in matrix notation

$$\dot{\gamma}^C_{App}=\mathbf{C}\dot{\gamma}+\frac{2\mathbf{D}\mathbf{v}_{slip}}{\mathbf{h}}=\mathbf{E}\mathbf{W}. \quad (11b)$$

Here $\mathbf{W}=\{\dot{\gamma}, \mathbf{v}_{slip}\}=\{\dot{\gamma}_1, \dot{\gamma}_2,\ldots\dot{\gamma}_{N_p}, v_{slip1}, v_{slip2},\ldots v_{slipN_p}\}$ is the composite column vector used to represent the two unknown discretized material property functions. $\mathbf{E}=\mathbf{C}+2\mathbf{D}/\mathbf{h}$ is the corresponding known composite matrix of coefficients with the understanding that the appropriate disk gap h_g from **h** is used in the evaluation of **E**. Evaluation of the matrices **C** and **D** are particularly simple, since these are the coefficients of linear interpolation of τ_{gi_M} between the elements of $\sigma=\{\sigma_1, \sigma_2,\ldots \sigma_{N_p}\}$. Thus for a given τ_{gi_M} all these coefficients vanish except for the two associated with the two elements of σ that bracket τ_{gi_M}.

As with Eq. (3), the elements of W are now chosen to minimize the linear combination of: (i) the sum of squares of $\dot{\gamma}_{App}-\dot{\gamma}^C_{gApp}$ and (ii) $\sum_{i_p=2}^{N_p-1}\left(\frac{d^2\dot{\gamma}}{d\tau^2}\right)^2_{i_p}+\sum_{i_p=2}^{N_p-1}\left(\frac{d^2v_{slip}}{d\tau^2}\right)^2_{i_p}$. This leads to, the equivalent of Eq. (6),

$$\mathbf{W}=\left(\mathbf{E}^T\mathbf{E}+\frac{\chi}{\Delta_\sigma^4}\beta^T\beta\right)^{-1}(\mathbf{E})^T. \quad (12)$$

Δ_σ is the uniform discretization interval of σ. The regularization parameter χ is again determined by GCV based on its equivalent of Eqs. (7) and (8).

Depending on the nature of the material under test, the minimum shear stress in each of the $\dot{\gamma}_{gApp}(\tau)$ curves may or may not be zero. For example, if the material has a yield stress τ_Y and a critical wall shear stress τ_{wcrit} below which wall slip is not observed then the lowest stress in $\dot{\gamma}_{gApp}(\tau)$ will be larger than zero. If either τ_Y or τ_{wcrit} or both are zero

then $\dot{\gamma}_{gApp}(\tau)$ will start from $\tau=0$. When either τ_Y or τ_{wcrit} or both are non-zero, the lower limit of $\sigma=\{\sigma_1, \sigma_2, \ldots \sigma_{Np}\}$ will have to be adjusted iteratively to satisfy the conditions

$$\dot{\gamma}(\tau_Y)=0 \tag{13}$$

and/or

$$v_{slip}(\tau_{wcrit})=0. \tag{14}$$

These provide the necessary equations for the determination of τ_Y and/or τ_{wcrit}.

5. Data and results

5.1. Oil-in-water emulsion

To demonstrate their technique for coping with wall slip, Yoshimura and Prud'homme (1988) obtained the $\dot{\gamma}_{gAppR}-\Gamma$ data, g=1 and 2, for a paraffin oil-in-water emulsion in a parallel disk-viscometer. Their data, reconstructed by scanning and digitizing of their original $\dot{\gamma}_{gAppR}-\Gamma$ plots, are shown as discrete points in Fig. 1(a). These data are for disks with R=26.85 mm and **h**={0.50, 0.75} mm. From the trend of the data it is assumed that $\Gamma\rightarrow 0$ as $\dot{\gamma}_{gAppR}\rightarrow 0$ for g=1 and 2. Because of the clustering of the data points at low $\dot{\gamma}_{gAppR}$, the reconstructed data in this region may have error bars larger than in the original data.

Applying Eq. (6) to the two sets of data in Fig. 1(a) resulted in the two $\tau(\dot{\gamma}_{gApp})$ curves shown as lighter curves in Fig. 1(b). For this emulsion, both curves pass through the origin of the plot. As explained above, without data extrapolation, this implies either τ_Y or τ_{wcrit} or both vanish.

In arriving at the two $\tau(\dot{\gamma}_{gApp})$ curves minimization of the GCV function was used to locate the appropriate λ. The GCV function for the data with h=0.5 mm is shown in Fig. 1(c). This curve is typical of the GCV functions encountered in this investigation. In all the computation reported in this paper the viscometry data have been made dimensionless prior to any Tikhonov regularization computation consequently the GCV function in Fig. 1(c) is also dimensionless. It should also be mentioned that the λ_{opt} depends not only on the noise level in the viscometry data but also on the number and distribution of the data points and the number of discretization points, therefore no physical significance should be associated with the numerical value of $\lambda_{opt}/\Delta^4\approx 865$.

Eq. (12) is now used to convert the two $\tau(\dot{\gamma}_{gApp})$ curves into material property functions. The $\dot{\gamma}(\tau)$ function is shown as a dark curve, in Fig. 1(d). The corresponding slip velocity function $v_{slip}(\tau_w)$ is shown in Fig. 1(e). In arriving at these curves the lower limit of τ, *i.e.*, τ_Y and that of τ_w, *i.e.*, τ_{wcrit} have been adjusted iteratively so that Eqs. (13) and (14) are met as closely as required. These led to $\tau_Y=$ 15.46 Pa and $\tau_{wcrit}=0$ for the oil-in-water emulsion. They imply that this emulsion slips before it undergoes shear deformation. Because of the uncertainty associated with the reconstructed parallel disk data at low apparent shear rates, the value of τ_Y should be treated only as an approximate estimate.

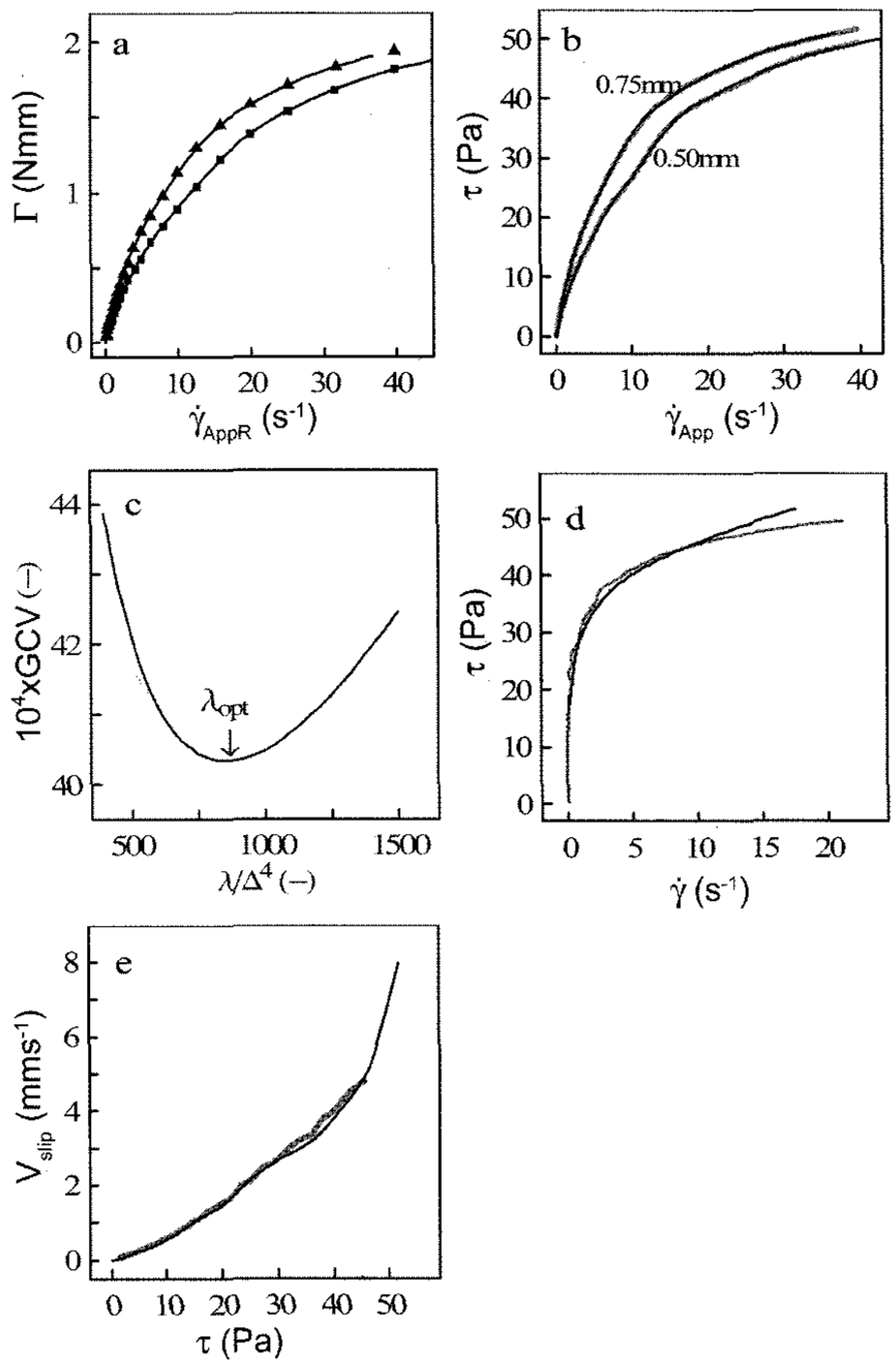

Fig. 1. Data and results of oil-in-water emulsion. (a) Apparent rim shear rate versus torque data for two different disk gaps. Points are the data from Yoshimura and Prud'homme (1988) and the curves is back calculated from the $\dot{\gamma}(\tau)$ and $v_{slip}(\tau_w)$ given by Eq. (12). Disk gap= 0.5 (■), 0.75 (▲) mm. (b) Shear stress-apparent shear rate curves. The lighter curves are from Eq. (6) and darker curves are back-calculated from $\dot{\gamma}(\tau)$ and $v_{slip}(\tau_w)$. (c) Dimensionless GCV function plot for the h=0.50 mm data showing $\lambda_{opt}/\Delta^4\approx 865$ (dimensionless). (d) Shear stress function. The lighter curve is from Yoshimura and Prud'homme (1988) and the darker curve is given by Eq. (12) showing $\tau_Y=15.46$ Pa. (e) Slip velocity function. The lighter curve is from Yoshimura and Prud'homme (1988) and the darker curve is given by Eq. (12).

For comparison, the shear stress function $\tau(\dot{\gamma})$ and the slip velocity function $v_{slip}(\tau_w)$ reported by Yoshimura and Prud'homme (1988), again reconstructed by scanning and digitization, are shown as lighter curves in Fig. 1(d) and (e), respectively. There is satisfactory agreement between the results from Yoshimura and Prud'homme (1988) and that obtained in this investigation. The lighter $v_{slip}(\tau_w)$ curve has to be thickened for it to show up. In Fig. 1(d), it can be seen that, close to $\dot{\gamma}=0$ the $\tau(\dot{\gamma})$ curve from Yoshimura and Prud'homme (1988) is nearly vertical indicating the existence

of a yield stress. They did not report a value for this stress.

As a further check of the reliability of the $\dot{\gamma}(\tau)$ and $v_{slip}(\tau_w)$ given by Eq. (12), they are used to back calculate the $\tau(\dot{\gamma}_{gApp})$ and also the $\dot{\gamma}_{gAppR}$–Γ relationship for the two disk gaps employed by Yoshimura and Prud'homme (1988). The back-calculated results are shown as continuous curves in Figs. 1(b) and 1(a), respectively. Very satisfactory agreement is observed in both figures. Again some of the lighter curves have to be thickened for them to show up in these comparisons. Since the back calculations were performed using commercial software that are independent of the computer codes developed in the present investigation they provide a useful check on the computation involved in Eqs. (6) and (12).

5.2. Shaving foam

As part of their investigation of wall slip and yielding in pasty materials, Bertola and coworkers (2003) reported the parallel disk data for a shaving foam. Their original data, in the form of $\dot{\gamma}_{gAppR}$ versus τ_R for g 1 to 7, are reproduced in Fig. 2(a). For $\dot{\gamma}_{gAppR}$ less than about 100 s^{-1}, the data for different disk gaps separate into distinct curves. This is taken as an indication that wall slip is observed under these conditions. A subset of their data, for four disk gaps, are used to test the performance of the two-step Tikhonov regularization procedure of Eqs. (6) and (12). The data used are marked out as darker points in Fig. 2(a). These data cover **h**={0.12, 0.2, 0.5, 0.75} mm. R=20 mm for all these data.

Before applying Eq. (6), the reported rim shear stress τ_R of the selected data points has to be converted back to applied torque Γ. This is done by the simple expression $\Gamma=\pi R^3\tau_R/2$ given by Eq. (4) after making the Newtonian assumption. The originator of the foam data, Coussot (2004), has been consulted on this conversion. The resulting $\dot{\gamma}_{gAppR}$–Γ data of the selected points are shown in Fig. 2(b) as discrete points.

Following the same procedure as in the previous example, Eq. (6) is used to convert the four sets of $\dot{\gamma}_{gAppR}$–Γ data into four separate $\tau(\dot{\gamma}_{gApp})$ curves. These are shown as lighter curves in Fig. 2(c). All these curves pass closely through the origin indicating that either τ_Y or τ_{wcrit} or both are zero.

Applying Eq. (12) to the four $\tau(\dot{\gamma}_{gApp})$ simultaneously resulted in the $\tau(\dot{\gamma})$ and $v_{slip}(\tau_w)$ in Figs. 2(d) and (e), respectively. Imposition of Eqs. (13) and (14) gave τ_Y= 12.25 Pa and $\tau_{wcrit}\approx 0$ indicating that this shaving foam also slips before it undergoes any shear deformation. The $\tau(\dot{\gamma})$ curve shows the classical shear thinning behaviour and is relatively smooth. The $v_{slip}(\tau_w)$ curve is not as smooth and the slip velocity shows sign of increasing rapidly with τ_w at high wall shear stress.

Again as in the previous example, the material property functions $\dot{\gamma}(\tau)$ and $v_{slip}(\tau_w)$ are used to back calculate the four $\tau(\dot{\gamma}_{gApp})$ curves and the $\dot{\gamma}_{gAppR}$–Γ relationships for the four disk gaps. The back-calculated results are shown as darker curves in Figs. 2(c) and (b), respectively. As τ_{wcrit}= 0, these back-calculated curves passes through the origin.

The material property functions $\dot{\gamma}(\tau)$ and $v_{slip}(\tau_w)$ given by Eq. (12) can be used to compute the behaviour of the foam in any disk geometry over the range of shear stress for which they have been defined. As a further test, they

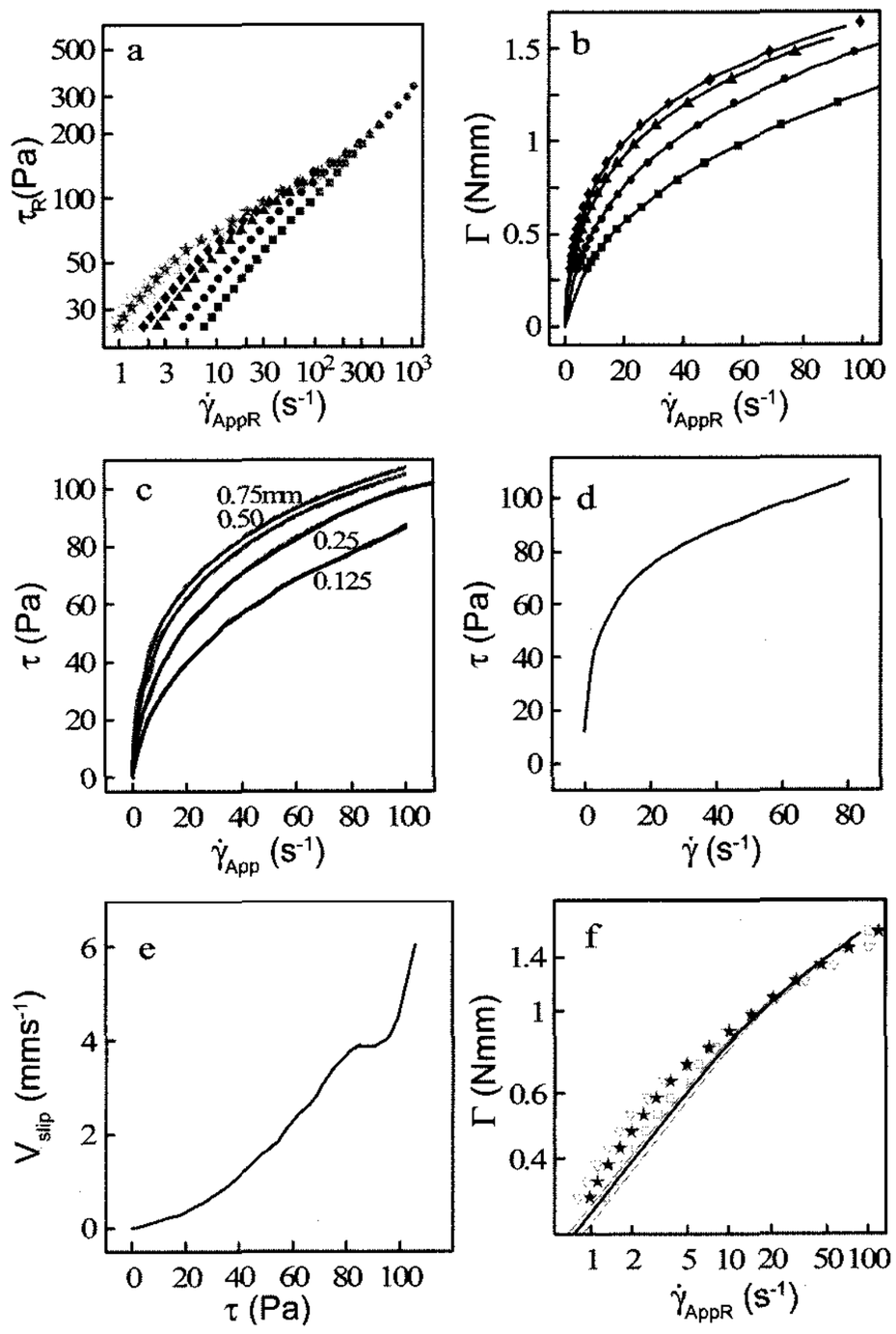

Fig. 2. Data and results of shaving foam. (a) Rim shear stress versus apparent rim shear rate data from Bertola and coworkers (2003) for disk gap=0.125(■), 0.25(●), 0.5(▲), 0.75(◆), 1.0(□), 1.25(★) and 1.5(▽) mm. Darker data points: used in Eq. (6) computation, lighter points: not used. (b) Apparent rim shear rate-torque curves. The discrete points are converted from selected data in Bertola and coworkers (2003) for disk gap=0.125(■), 0.25(●), 0.5(▲), 0.75(◆) mm and the curves are back calculated from the $\dot{\gamma}(\tau)$ and $v_{slip}(\tau_w)$ given by Eq. (12). (c) Shear stress-apparent shear rate curves. The lighter curves are from Eq. (6) and the darker curves are back calculated using $\dot{\gamma}(\tau)$ and $v_{slip}(\tau_w)$. (d) The shear stress function given by Eq. (12) showing τ_Y=12.25 Pa. (e) The slip velocity function given by Eq. (12). (f) Apparent rim shear rate-torque curves for large disk gaps. The discrete points are converted from the data from Bertola and coworkers (2003) for h=1.0(□), 1.25(★) and 1.5(▽) mm. The thicker curve is for h=1.25 mm back calculated from $\dot{\gamma}(\tau)$ and $v_{slip}(\tau_w)$ and the finer curves to the left and right are the back-calculated curves for h=1.5 and 1 mm, respectively.

are used here to compute the Γ for **h** = {1, 1.25, 1.5} mm, *i.e.*, the three larger disk gaps in the data in Bertola and coworkers (2003) that were not used in the Tikhonov regularization computation of Eqs. (6) and (12). The resulting $\dot{\gamma}_{gAppR}$ –Γ are shown as continuous curves in Fig. 2(f). As expected these curves are very close to one another. For comparison, the large disk gap $\dot{\gamma}_{gAppR}$ –Γ data from the original measurements in Bertola and coworkers (2003) are shown as discrete points on the same plot. This comparison is presented in log-log format to reveal the differences observed at low $\dot{\gamma}_{gAppR}$. As expected, the agreement of the computed torque with the original data is less satisfactory compared to that observed in Fig. 2(b). It is also noted that some of the original large disk gap torque data points do not follow the trend described by Eq. (9) where, for any rim shear stress (and hence torque), $\dot{\gamma}_{gAppR}$ is expected to decrease monotonically as h is increased. Clearly the simple relationship given by Eq. (9) does not describe the rheology of the shaving foam in question over the entire range of the experimental observations.

5.3. Coleslaw mayonnaise

It is generally agreed that mayonnaise is a shear thinning material with a yield stress and may exhibit wall slip under certain conditions. This makes rheological characterization of mayonnaise difficult, even under steady-state conditions, as noted by Plucinski and coworkers (1998). To test the performance of Eqs. (6) and (12), a rudimentary parallel-disk viscometer is used to obtain the $\dot{\gamma}_{gAppR}$ –Γ data of a mayonnaise (Kraft Classic Coleslaw) bought from a supermarket. These data are shown as discrete points in Fig. 3(a). R = 12 mm and **h** = {0.65, 1.55, 2.85} mm for these data. The sensitivity of the viscometer used does not permit the determination of the torque much below those included in this figure.

The $\tau(\dot{\gamma}_{gApp})$ curves, g = 1 to 3, given directly by Eq. (6) for this mayonnaise are shown as lighter curves in Fig. 3(b). The vertical intercepts of these curves, *i.e.*, $\tau(\dot{\gamma}_{gApp} = 0)$ = {17.29, 13.27, 12.31} Pa for g = 1, 2 and 3. These non-zero intercepts can be taken as an indication that this mayonnaise has either a τ_Y or a τ_{wcrit} or both. The spread of these intercepts is a measure of the uncertainty in $\tau(\dot{\gamma}_{gApp} = 0)$.

Application of Eq. (12) to the three $\tau(\dot{\gamma}_{gApp})$ curves simultaneously led to the material property functions $\dot{\gamma}(\tau)$, plotted as stress function, in Fig. 3(c) and $v_{slip}(\tau_w)$ in Fig. 3(d). Iterative computation of Eqs. (13) and (14) gave τ_Y = 20.60 Pa and τ_{wcrit} = 17.25 Pa. Thus this mayonnaise also slips before it deforms under steady shear.

The $\dot{\gamma}(\tau)$ and $v_{slip}(\tau_w)$ of the mayonnaise are again used to back calculate the $\tau(\dot{\gamma}_{gApp})$ curves and the outcome are shown as the darker curves in Fig. 3(b). These are in good agreement with the lighter curves given directly by Eq. (6). Similarly the back-calculated $\dot{\gamma}_{gAppR}$ –Γ for the three disk gaps are shown in Fig. 3(a) for comparison with the original viscometry data. The non-zero τ_Y and τ_{wcrit} show up as finite intercepts in the $\tau(\dot{\gamma}_{gApp})$ and $\dot{\gamma}_{gAppR}$ –Γ plots in Figs. 3(a) and (b).

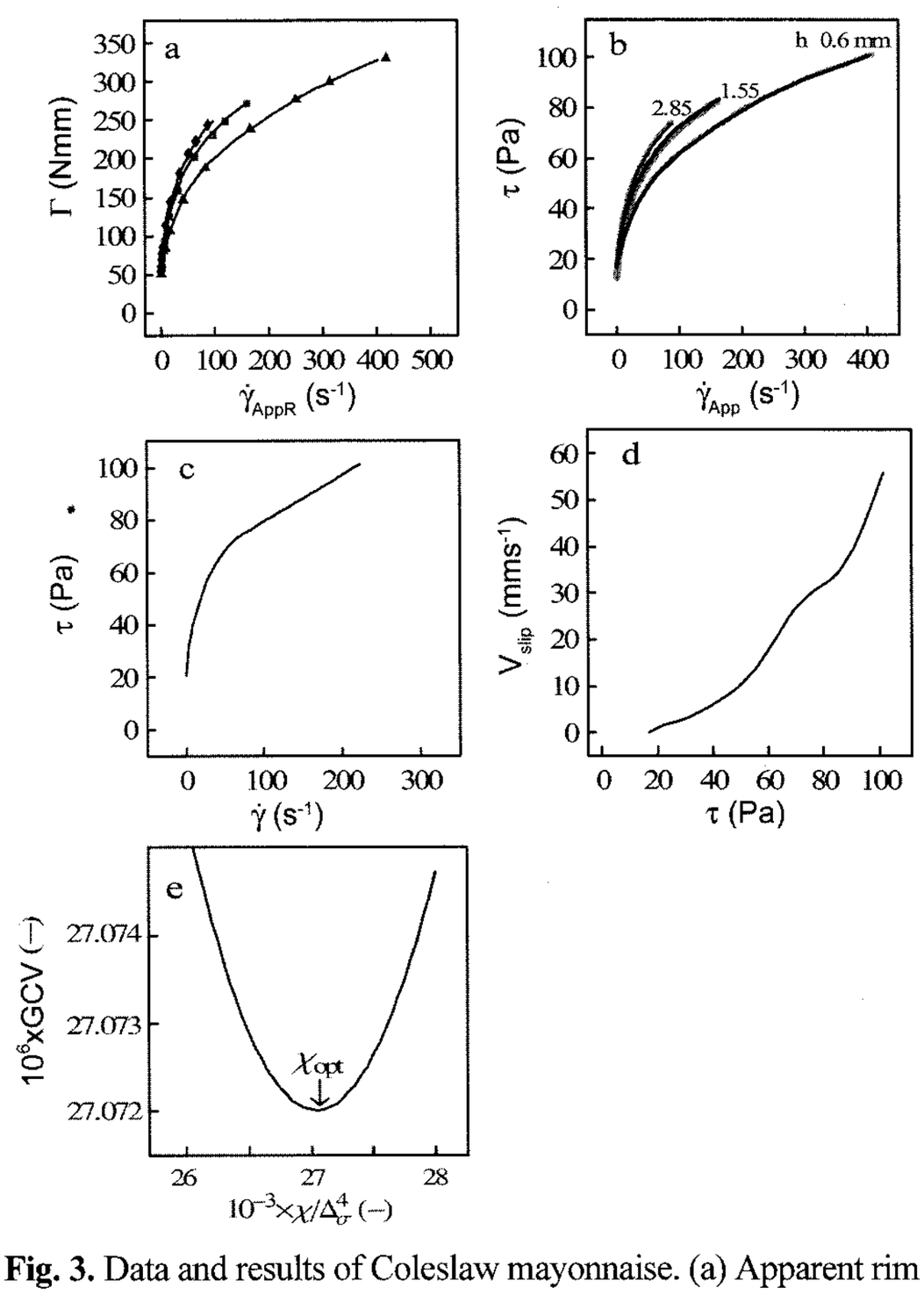

Fig. 3. Data and results of Coleslaw mayonnaise. (a) Apparent rim shear ratetorque curves. The discrete points are experimental data for disk gap = 0.6(▲), 1.55(■) and 2.85(◆) mm. The curves are back calculated from the $\dot{\gamma}(\tau)$ and $v_{slip}(\tau_w)$ given by Eq. (12). (b) Apparent shear stress-apparent shear rate curves. The lighter curves are from Eq. (6) and darker curves are back calculated using $\dot{\gamma}(\tau)$ and $v_{slip}(\tau_w)$. (c) The shear stress function given by Eq. (12) showing τ_Y = 20.60 Pa. (d) Slip velocity function given by Eq. (12) showing τ_{wcrit} = 17.25 Pa. (e) Dimensionless GCV function plot for Eq. (12) showing $\chi_{opt}/\Delta_\sigma^4$ ≈27050 (dimensionless).

The dimensionless GCV function used to guide the choice of the regularization parameter χ associated with Eq. (12) for the mayonnaise is shown in Fig. 3(e). Again no physical significance should be read into the numerical value of $\chi_{opt}/\Delta_\sigma^4$ ≈27050 (dimensionless).

6. Discussion

The three examples considered here show how the two-step Tikhonov regularization procedure can be applied to convert general multi-gap parallel disk data into material property functions. They also reveal some of the advan-

tages of this method. The method is able to extract the maximum amount of information hidden in a given set of parallel disk data. Apart from the assumption that $\tau(\dot{\gamma})$ and $v_{slip}(\tau_w)$ are well behaved functions, the method does not require the imposition of specific expressions to describe the expected rheological behavior of the material under test. If the material has a τ_Y or a τ_{wcrit}, iterative calculations will give an estimate of these stresses.

In this investigation, computation of the GCV function was used to guide the selection of the regularization parameters λ and χ. These are the most time consuming steps in the entire Tikhonov regularization computing process. Depending on the number of data points and the number of disk gaps involved they each can take as much as 5 to 10 minutes on a 3 GHz PC. While this is quite acceptable, such computation can be avoided. Instead of GCV, the simpler Morozov Principle can be used to guide the choice of both of these parameters. Guided by general knowledge of the error bars of the data and, more importantly, by the expected physical behaviour of the material property functions, it is quite possible to arrive at the appropriate choice of these parameters after only a small number of exploratory computation runs. The resulting material property functions are not very sensitive to small changes in these parameters therefore fine tuning of λ and χ are generally not required.

Examination of the shear stress versus apparent shear rate curves in Figs. 1(b), 2(b) and 3(b) shows clearly that the shear stress is significantly nonlinear over the range of the apparent shear rate $\dot{\gamma}_{App}$ covered in each experimental run. By definition, $\dot{\gamma}_{App} = \omega r/h$ is linear in r hence the shear stress is also significantly non-linear in r. Consequently the use of the Newtonian approximation to convert the measured torque Γ into a rim shear stress τ_R is likely to incur significant error. This error will, in turn, introduce considerable uncertainty in the wall slip velocity function whether it is obtained by the procedure of Yoshimura and Prod'homme for two-gap data or the Mooney method or the present Tikhonov regularization method for multi-gap data. It is interesting to note that in their original work Yoshimura and Prud'homme (1988) used the exact Eq. (4) to perform the conversion between torque and rim shear stress.

7. Conclusion

The two-step Tikhonov regularization procedure provides a reliable method for converting multi-gap steady shear data from parallel-disk viscometers into shear stress function and slip velocity function. For materials with a yield stress or a critical wall shear stress the procedure will provide an estimate of these stresses. GCV function can be used to guide the selection of the regularization parameters. The Morozov Principle provides a computationally less intensive alternative method for choosing these parameters.

Acknowledgements

The authors thank Prof. Coussot for the computer file containing the steady shear data from Fig. 1. of his paper and for his advice regarding the conversion between rim shear stress and torque.

References

Bertola, V., F. Bertrand, H. Tabuteau, D. Bonn and P. Coussot, 2003, Wall slip and yielding in pasty materials, *J. Rheol.* **47**, 1211-1226.

Brunn, P. O., 1998, A note on the slip velocity concept for purely rotational viscometric flows, *Rheol. Acta* **37**, 196-197.

Coussot, P., 2004, Private Communication.

Engl, H. W., M. Hanke and A. Neubauer, 2000, *Regularization of Inverse Problems*, Kluwer, Dordrecht.

Kiljañski, T., 1989, A method for correction of the wall-slip effect in a Couette rheometer, *Rheol. Acta* **28**, 61-64.

Macosko, C. W., 1994, *Rheology: Principles, Measurements and Applications*, VCH, New York.

Mooney, M., 1931, Explicit formulas for slip and fluidity, *J. Rheol.* **2**, 210-222.

Plucinski, J., R. K. Gupta and S. Chakrabarti, 1998, Wall slip of mayonnaises in viscometers, *Rheol. Acta* **37**, 256-269.

Schlegel, D., 1980, Bestimmung der schubspannungsfunktion des blutes mit dem Couette-rheometer unter Berücksichtigung des wandverhaltens, *Rheol. Acta* **19**, 375-380.

Shipman, R. W. G., M. M. Denn and R. Keunings, 1991, Free-surface effects in torsional parallel-plate rheometry, *Ind. Eng. Chem. Res.* **30**, 918-922.

Wahba, G., 1990, *Spline Models for Observational Data*, SIAM, Philadelphia.

Wein, O. and V. V. Tovchigrechko, 1992, Rotational viscometry under presence of apparent wall slip, *J. Rheol.* **36**, 821-844.

Yeow, Y. L., H. L. Lee, A. R. Melvani and G. C. Mifsud, 2003, A new method of processing capillary viscometry data in the presence of wall slip, *J. Rheol.* **47**, 337-348.

Yeow, Y. L., B. Choon, L. Karniawan and L. Santoso, 2004, Obtaining the shear rate function and the slip velocity function from Couette viscometry data, *J. Non-Newtonian Fluid Mech.* **124**, 43-49.

Yeow, Y. L., D. Chandra, A. A. Sardjono, H. Wijaya, Y. K. Leong and A. Khan, 2005, A general method for obtaining shear stress and normal stress functions from parallel disk rheometry data, *Rheol. Acta* **44**, 270-277.

Yeow, Y. L., Y. K. Leong and A. Khan, 2006, Non-Newtonian flow in parallel-disk viscometers in the presence of wall slip, *J. Non-Newtonian Fluid Mech.* **139**, 85-92.

Yeow, Y. L., Y. K. Leong and A. Khan, 2007, Error introduced by a popular method of processing parallel-disk viscometery data, *Appl. Rheol.* **17**, 66415-1-66415-6.

Yoshimura, A. and R. K. Prud'homme, 1988, Wall slip corrections for Couette and parallel disk viscometers, *J. Rheol.* **32**, 53-67.